Inorganic Chemistry

ARTICLE

pubs.acs.org/IC

Novel Yellow-Emitting $Sr_8MgLn(PO_4)_7:Eu^{2+}$ (Ln = Y, La) Phosphors for Applications in White LEDs with Excellent Color Rendering Index

Chien-Hao Huang and Teng-Ming Chen*

Phosphors Research Laboratory and Department of Applied Chemistry, National Chiao Tung University, Hsinchu 30010, Taiwan

Supporting Information

ABSTRACT: Eu^{2+}-activated $Sr_8MgY(PO_4)_7$ and $Sr_8MgLa(PO_4)_7$ yellow-emitting phosphors were successfully synthesized by solid-state reactions for applications in excellent color rendering index white light-emitting diodes (LEDs). The excitation and reflectance spectra of these phosphors show broad band excitation and absorption in the 250−450 nm near-ultraviolet region, which is ascribed to the $4f^7 \rightarrow 4f^65d^1$ transitions of Eu^{2+}. Therefore, these phosphors meet the application requirements for near-UV LED chips. Upon excitation at 400 nm, the $Sr_8MgY(PO_4)_7:Eu^{2+}$ and $Sr_8MgLa(PO_4)_7:Eu^{2+}$ phosphors exhibit strong yellow emissions centered at 518, 610, and 611 nm with better thermal stability than $(Ba,Sr)_2SiO_4$ (570 nm) commodity phosphors. The composition-optimized concentrations of Eu^{2+} in $Sr_8MgLa(PO_4)_7:Eu^{2+}$ and $Sr_8MgY(PO_4)_7:Eu^{2+}$ phosphors were determined to be 0.01 and 0.03 mol, respectively. A warm white-light near-UV LED was fabricated using a near-UV 400 nm chip pumped by a phosphor blend of blue-emitting $BaMgAl_{10}O_{17}:Eu^{2+}$ and yellow-emitting $Sr_8MgY(PO_4)_7:0.01Eu^{2+}$ or $Sr_8MgLa(PO_4)_7:0.03Eu^{2+}$, driven by a 350 *m*A current. The $Sr_8MgY(PO_4)_7:0.01Eu^{2+}$ and $Sr_8MgLa(PO_4)_7:0.03Eu^{2+}$ containing LEDs produced a white light with Commission International de l'Eclairage (CIE) chromaticity coordinates of (0.348, 0.357) and (0.365, 0.328), warm correlated color temperatures of 4705 and 4100 K, and excellent color rendering indices of 95.375 and 91.75, respectively.

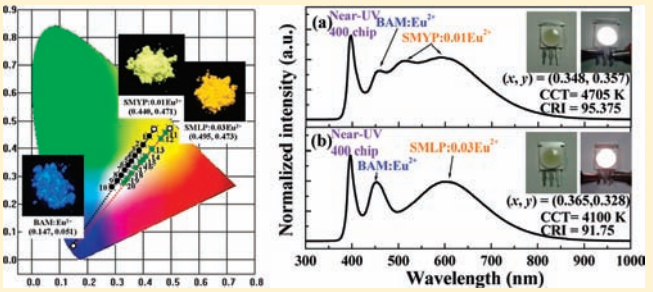

1. INTRODUCTION

In recent years, white light-emitting diodes (LEDs) have attracted much attention because of their high efficiency, compactness, good material stability, long operational lifetime, and resultant energy savings.[1−3] The applications of these LEDs include lighting sources and backlit automobile lamps.[4−6] Nowadays, the majority of white LEDs use a blue InGaN chip pumped with yellow-emitting $Y_3Al_5O_{12}:Ce^{3+}$ (YAG:Ce^{3+}) phosphors.[7] They are characterized by cool white light with Commission International de l'Eclairage (CIE) chromaticity coordinates of (0.292, 0.325), a correlated color temperature (CCT) of 7756 K, and poor color rendering indices (CRI, *Ra*) of 75.[8] However, their lack of red-light contribution restricts their use in more vivid applications.[9] Recently, white LEDs fabricated using near-ultraviolet chips (380−420 nm) coupled with a blend of yellow- and blue-emitting phosphors have exhibited favorable properties, including tunable CCTs, tunable CIE chromaticity coordinates, and excellent *Ra* values. Therefore, it is important to develop new yellow-emitting phosphors for near-UV LED applications. The luminescence of Eu^{2+}-activated phosphors is characterized by intense broad band absorption in the ultraviolet (350−380 nm) or near-ultraviolet (380−420 nm) regions and an emission wavelength that can be tuned from ultraviolet to red. The intense broad band absorption and emission were assigned to the 4f-5d dipole-allowed electronic transitions of the Eu^{2+} ions. Many yellow-emitting phosphors with Eu^{2+} activated for near-UV LEDs have been reported, including $Sr_3B_2O_6:Eu^{2+}$,[10] $LiSrBO_3:Eu^{2+}$,[11] $Ca_2BO_3Cl:Eu^{2+}$,[12] $Li_2SrSiO_4:Eu^{2+}$,[13] $Sr_2SiO_4:Eu^{2+}$,[14] $Ca_3SiO_4Cl_2:Eu^{2+}$,[15] $Ba_2Mg(PO_4)_2:Eu^{2+}$,[16] and $Sr_3(Al_2O_5)Cl_2:Eu^{2+}$.[17]

To the best of our knowledge, the crystal structures and luminescence properties of $Sr_8MgY(PO_4)_7:xEu^{2+}$ and $Sr_8MgLa(PO_4)_7:yEu^{2+}$ have not yet been reported in the literature. In this study, we investigated the luminescence properties of yellow-emitting $Sr_8MgY(PO_4)_7:xEu^{2+}$ and $Sr_8MgLa(PO_4)_7:yEu^{2+}$ phosphors. In addition, white-light near-UV LEDs possessing excellent CRI values and warm correlated color temperatures were fabricated using phosphor blends of blue-emitting $BaMgAl_{10}O_{17}:Eu^{2+}$ and yellow-emitting $Sr_8MgY(PO_4)_7:0.01Eu^{2+}$ or $Sr_8MgLa(PO_4)_7:0.03Eu^{2+}$ and their optical properties were investigated.

2. EXPERIMENTAL SECTION

2.1. Materials and Synthesis. Polycrystalline phosphors with compositions of $(Sr_{1-x}Eu_x)_8MgY(PO_4)_7$ (SMYP:xEu^{2+}) and $(Sr_{1-y}Eu_y)_8MgLa(PO_4)_7$ (SMLP:yEu^{2+}) described in this work were prepared with a high-temperature solid-state reaction. Briefly, the constituent raw materials $SrCO_3$ (A. R., 99.9%), MgO (A. R., 99%), Y_2O_3 (A. R., 99.99%) or La_2O_3 (A. R., 99.9%), $(NH_4)_2HPO_4$ (Merck ≥99%), and Eu_2O_3

Received: March 12, 2011
Published: May 18, 2011

(A. R., 99.99%) were weighed in the following stoichiometric molar ratios: $8(1-x)$ or $8(1-y)$:1:1/2:7: x or y (x = 0−0.05, y = 0−0.05 mol) and thoroughly ground thoroughly in an agate mortar, and the homogeneous mixture was transferred to an alumina crucible and calcined in a furnace at ∼1573 K for 8 h under a reducing atmosphere of 15% H_2/85% N_2.

2.2. Materials Characterization. All crystal structure compositions were checked for phase formation by using powder X-ray diffraction (XRD) analysis with a Bruker AXS D8 advanced automatic diffractometer with Cu Kα radiation (λ = 1.5418 Å), over the angular range $10° \le 2\theta \le 80°$, operating at 40 kV and 40 *m*A. The photoluminescence (PL) and photoluminescence excitation (PLE) spectra of the samples were analyzed by using a Spex Fluorolog-3 Spectrofluorometer equipped with a 450 W Xe light source. The Commission International de l'Eclairage (CIE) chromaticity coordinates for all samples were measured by a Laiko DT-101 color analyzer equipped with a CCD detector (Laiko Co., Tokyo, Japan). Diffuse reflectance spectra of phosphor samples were measured with a Hitachi 3010 double-beam UV−visible (vis) spectrometer (Hitachi Co., Tokyo, Japan) equipped with a Ø60 mm integrating sphere whose inner face was coated with $BaSO_4$ or Spectralon, and α-Al_2O_3 was used as a standard in the measurements. Thermal quenching measurements were investigated using a heating apparatus (THMS-600) in combination with the PL equipment.

2.3. LED Lamp Fabrication. White LED lamps were fabricated by integrating a mixture of transparent silicon resin and phosphors blend of yellow-emitting $Sr_8MgY(PO_4)_7$:0.01Eu^{2+} or $Sr_8MgLa(PO_4)_7$:0.03Eu^{2+} and blue-emitting $BaMgAl_{10}O_{17}$:Eu^{2+} commodity on an 400 near-UV chip (AOT Product No: C06HC, Spec: 400 V10C, wavelength peak: 395−400 ± 1.32 nm, chip size: 40 × 40 mil, VF1: 3.8−4.0 ± 0.06 V, IV1: 90−100 ± 2.65 *m*W) and roast at 120 °C/10 h afterward.

3. RESULTS AND DISCUSSION

3.1. Crystal Structure and Composition Analysis. The compounds $Sr_8MgY(PO_4)_7$:xEu^{2+} (SMYP:xEu^{2+}) and $Sr_8MgLa(PO_4)_7$:yEu^{2+} (SMLP:yEu^{2+}) are isostructural with $Sr_9In(PO_4)_7$. The synchrotron X-ray powder diffraction data of $Sr_9In(PO_4)_7$, reported by Belik et al.,[18] reveals that the crystal structure of $Sr_9In(PO_4)_7$ has a monoclinic space group *I*2/*a* (No. 15, cell choice 3) and cell parameters of a = 18.0425(2) Å, b = 10.66307(4) Å, c = 18.3714(2) Å, β = 132.9263(5)°, V = 2588.02(4) Å^3, and N = 4. In the structures of both $Sr_8MgY(PO_4)_7$:xEu^{2+} and $Sr_8MgLa(PO_4)_7$:yEu^{2+}, the Sr^{2+} ions have five different coordination environments. Sr(1) is defined as being eight-coordinated; Sr(2), Sr(3), and Sr(4) are defined as being nine-coordinated; and Sr(5) is defined as being ten-coordinated. The ionic radii of the eight-, nine-, and ten-coordinated Sr^{2+} ions are 1.26, 1.31, and 1.36 Å, respectively. Similarly, the ionic radii of the eight-, nine-, and ten-coordinated Eu^{2+} ions are 1.25, 1.3, and 1.35 Å, respectively. Because of the similarities of their ionic radii, the Eu^{2+} ions are expected to randomly occupy Sr^{2+} ion sites in the $Sr_8MgY(PO_4)_7$:xEu^{2+} or $Sr_8MgLa(PO_4)_7$:yEu^{2+} crystal structure. Two series of phosphors with phase identifications of SMYP:0.05Eu^{2+} and SMLP:0.05Eu^{2+} were analyzed via X-ray diffraction (XRD), as portrayed in the profile shown in Figure 1. It was clearly observed that no detectable impurities were present in SMYP:0.05Eu^{2+} and SMLP:0.05Eu^{2+}. All XRD patterns were found to agree well with the standard data in the Inorganic Crystal Structure Database (ICSD 59722),[19] indicating that the doped Eu^{2+} ions did not generate any impurities or induce significant changes in the host structure. The chemical compositions of $Sr_8MgY(PO_4)_7$:0.05Eu^{2+} and $Sr_8MgLa(PO_4)_7$:0.05Eu^{2+} phosphors were analyzed by the

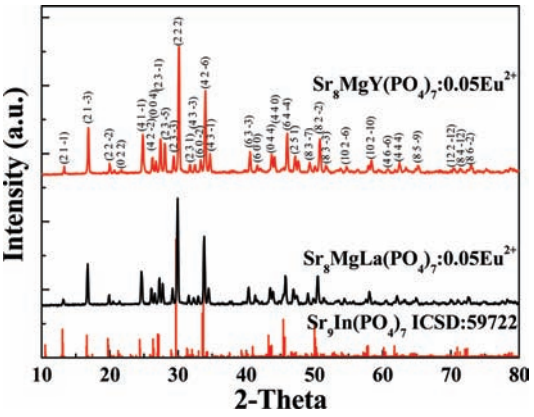

Figure 1. Powder XRD patterns of $Sr_9In(PO_4)_7$ standard pattern (ICSD 59722), $Sr_8MgY(PO_4)_7$:0.05Eu^{2+} and $Sr_8MgLa(PO_4)_7$:0.05Eu^{2+}.

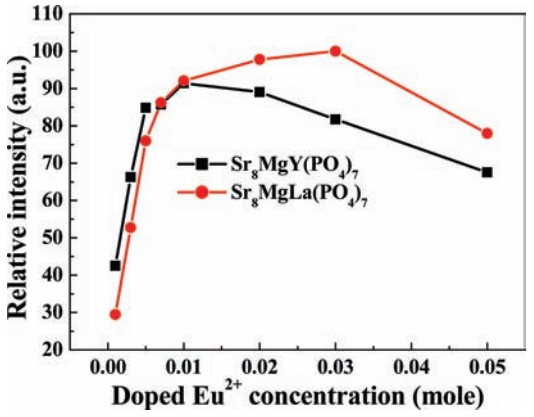

Figure 2. Concentration dependence of the relative emission intensity of $Sr_8MgY(PO_4)_7$:xEu^{2+} (x = 0.001−0.05) and $Sr_8MgLa(PO_4)_7$:yEu^{2+} (y = 0.001−0.05) phosphors under 400 nm excitation.

energy dispersive spectrometry (EDS) (see Supporting Information, Figure S1). Major chemical elements, namely Sr, Mg, Y(La), and P were determined from EDS data and atomic percentages of $Sr_8MgY(PO_4)_7$:0.05Eu^{2+} and $Sr_8MgLa(PO_4)_7$:0.05Eu^{2+} phosphors were found to be Sr:Mg:Y:P:Eu = 14.24:1.85:1.91:12.89:0.76 and Sr:Mg:La:P:Eu = 12.68:1.64:1.58: 11.72:0.66 (average values of ten analyses), respectively. Besides O composition, other atomic percentages matched well with those of $Sr_8MgY(PO_4)_7$:0.05Eu^{2+} and $Sr_8MgLa(PO_4)_7$:0.05Eu^{2+} phosphors. The atomic percentage ratio of O concentration was slightly higher than the expected value, which was due to the environmental trace and combustible gases evolved during the reaction.[20]

3.2. Photoluminescence Properties. Figure 2 shows the concentration dependence of the emission intensity of SMYP:xEu^{2+} and SMLP:yEu^{2+} with various concentrations of Eu^{2+} ions under 400 nm excitation. For SMYP:xEu^{2+} phosphors, the photoluminescence (PL) intensity increases with the increase in Eu^{2+} content up to a maximum x value of about 0.01 mol, after which it decreases because of interactions between Eu^{2+} ions. For SMLP:yEu^{2+} phosphors, the optimal doping concentration was observed to be 0.03 mol, and the PL intensity was observed to increase with increasing y when y < 0.03. For samples with Eu^{2+} dopant content higher than 0.03 mol, concentration quenching was observed, and the PL intensity decreased with

dx.doi.org/10.1021/ic200515w |*Inorg. Chem.* 2011, 50, 5725–5730

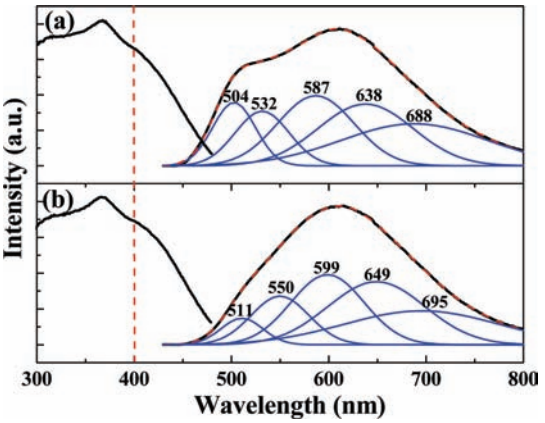

Figure 3. PL/PLE spectra of (a) $Sr_8MgY(PO_4)_7$:0.01Eu^{2+} (λ_{ex}:400 nm, λ_{em}:610 nm) and (b) $Sr_8MgLa(PO_4)_7$:0.03Eu^{2+} (λ_{ex}:400 nm, λ_{em}:611 nm) phosphors, fitted curve (red dashed line) and deconvoluted Gaussian components (blue solid lines).

increasing Eu^{2+} dopant content. According to the percolation model,[21,22] concentration quenching of the compound can occur by two mechanisms: (1) Interactions between the Eu^{2+} ions, which results in energy reabsorption among neighboring Eu^{2+} ions in the rare earth sublattice; (2) Energy transfer from a percolating cluster of Eu^{2+} ions to killer centers. Upon excitation at a wavelength of 400 nm, the internal quantum efficiencies (QEs) of composition-optimized SMYP:0.01Eu^{2+}, SMLP:0.03Eu^{2+} and commercial $(Sr,Ba)_2SiO_4$:Eu^{2+} (570 nm) phosphor were found to be 34.8%, 31.6%, and 90.4%, and the corresponding absorptions are 69.4%, 71.1%, and 81.6%. The external QEs of SMYP:0.01Eu^{2+}, SMLP:0.03Eu^{2+}, and $(Sr,Ba)_2SiO_4$:Eu^{2+} (570 nm) phosphor are determined to be 24.2%, 22.5%, and 73.8%, respectively. However, QEs of SMYP:0.01Eu^{2+} and SMLP:0.03Eu^{2+} are 32.7% and 30.5% of that of $(Sr,Ba)_2SiO_4$:Eu^{2+} (570 nm) phosphor, respectively. The observed low QEs of SMYP:0.01Eu^{2+} and SMLP:0.03Eu^{2+} can be further improved by process optimization.

Figure 3 illustrates the PL/PLE spectra of SMYP:0.01Eu^{2+}, SMLP:0.03Eu^{2+}, and the deconvoluted Gaussian components. The PLE spectrum has a broad hump between 250 and 470 nm, which is attributed to the $4f^7 \rightarrow 4f^65d^1$ transition of the Eu^{2+} ions. The broad excitation band matches well with the range of the near-UV LED chip (380−420 nm). The PL spectra of the SMYP:0.01Eu^{2+} and SMLP:0.03Eu^{2+} phosphors show broad yellow-emitting bands from 450 to 800 nm centered at 518, 610, and 611 nm, which were attributed to the $4f^65d^1 \rightarrow 4f^7$ transition of the Eu^{2+} ions. By Gaussian deconvolution, the PL spectra of the SMYP:0.01Eu^{2+} and SMLP:0.03Eu^{2+} phosphors can be decomposed into five Gaussian profiles with peaks centered at 504 nm (19,841 cm^{-1}), 532 nm (18,797 cm^{-1}), 587 nm (17,036 cm^{-1}), 638 nm (15,674 cm^{-1}), and 688 nm (14,535 cm^{-1}) (Figure 3a, blue solid lines) and 511 nm (19,569 cm^{-1}), 550 nm-(18,182 cm^{-1}), 599 nm(16,694 cm^{-1}), 649 nm(15,408 cm^{-1}), and 695 nm (14,388 cm^{-1}) (Figure 3b, blue solid lines), respectively. These peaks can be ascribed to five different emission sites, which could be identified as the different coordination environments of the Sr^{2+} ions being occupied by Eu^{2+} ions.[23]

3.3. Reflectance Spectra Properties. The reflectance spectra of $Sr_8MgY(PO_4)_7$:xEu^{2+} (x = 0−0.05) and $Sr_8MgLa(PO_4)_7$:yEu^{2+} (y = 0−0.05) were shown in Figure 4. The SMYP and SMLP host material shows energy absorption in the ≤340 nm region, and

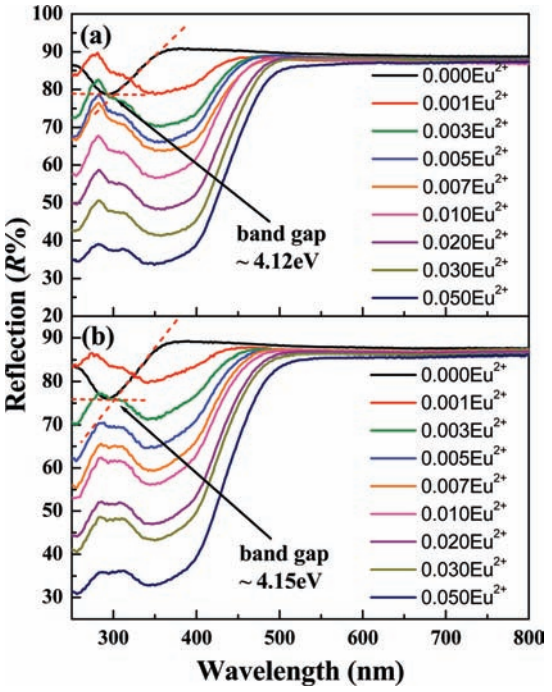

Figure 4. Reflectance spectra of (a) $Sr_8MgY(PO_4)_7$:xEu^{2+} (x = 0−0.05) and (b) $Sr_8MgLa(PO_4)_7$:yEu^{2+} (y = 0−0.05) phosphors.

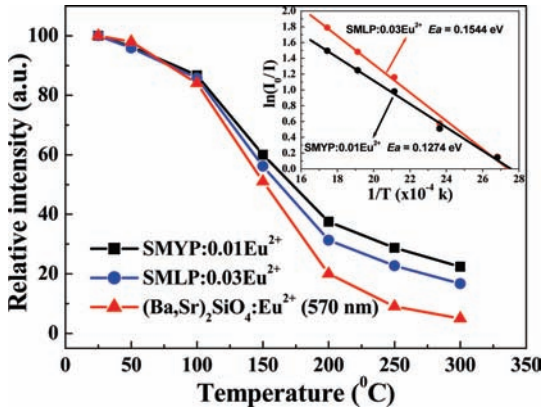

Figure 5. Temperature dependence of the relative emission intensity as a function of temperatures of $Sr_8MgY(PO_4)_7$:0.01Eu^{2+} and $Sr_8MgLa(PO_4)_7$:0.03Eu^{2+} and commercial $(Sr,Ba)_2SiO_4$:Eu^{2+} (570 nm) phosphors excited at 400 nm. The inset shows the activation energy (E_a) of the $Sr_8MgY(PO_4)_7$:0.01Eu^{2+} and $Sr_8MgLa(PO_4)_7$:0.03Eu^{2+} phosphors.

the band gaps were estimated to be about 4.12 eV (301 nm, Figure 4a) and 4.15 eV (299 nm, Figure 4b), respectively. As Eu^{2+} ions were doped into the SMYP or SMLP host,[24] a strong broad absorption appeared in the 250−450 nm near-UV range, which was assigned to the $4f^7 \rightarrow 4f^65d^1$ absorption of the Eu^{2+} ions. The absorption edge gradually extends to longer wavelengths, and the absorption is enhanced for higher Eu^{2+} ion concentrations; this results in an overall red shift of the excitation wavelength to 450 nm. For the SMYP:xEu^{2+} and SMLP:yEu^{2+} phosphors, the optimal Eu^{2+} dopant contents were found to be 0.01 and 0.05 mol, respectively. The SMYP:0.01Eu^{2+} and SMLP:0.03Eu^{2+} phosphors have a strong absorption range from

dx.doi.org/10.1021/ic200515w |Inorg. Chem. 2011, 50, 5725–5730

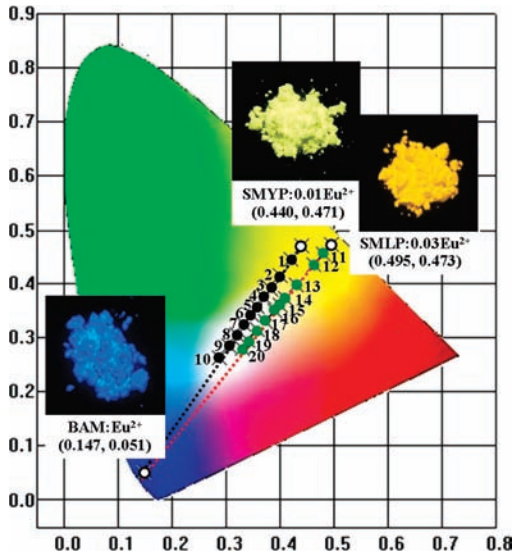

Figure 6. CIE chromaticity diagram of a mixing of $Sr_8MgY(PO_4)_7$:$0.01Eu^{2+}$ and $BaMgAl_{10}O_{17}$:Eu^{2+} phosphors (points 1−10) and $Sr_8MgLa(PO_4)_7$:$0.01Eu^{2+}$ and $BaMgAl_{10}O_{17}$:Eu^{2+} phosphors (points 11−20) with different weight ratios under 400 nm excitation.

250 to 450 nm, which matches well with near-UV chips for applications in white-light near-UV LEDs.

3.4. Thermal Quenching Properties. The thermal stability of phosphors is very important for high power LED applications. The temperature-dependent relative emission intensities of SMYP:$0.01Eu^{2+}$ and SMLP:$0.03Eu^{2+}$ phosphors and of commercial $(Ba,Sr)_2SiO_4$:Eu^{2+} (570 nm) phosphors under excitation at 400 nm are compared in Figure 5. The relative emission intensities of all phosphors decrease with increasing temperature in the range of 25 °C−300 °C. We observed a decay of 40% for SMYP:$0.01Eu^{2+}$, 43.8% for SMLP:$0.03Eu^{2+}$, and 49% for $(Ba,Sr)_2SiO_4$:Eu^{2+} (570 nm) at 150 °C. At 250 °C, decays of 71.3% for SMYP:$0.01Eu^{2+}$, 77.3% for SMLP:$0.03Eu^{2+}$, and 91% for $(Ba,Sr)_2SiO_4$:Eu^{2+} (570 nm) were observed. The thermal stability of the SMYP:$0.01Eu^{2+}$ and SMLP:$0.03Eu^{2+}$ phosphors above 250 °C were higher than that of the commercially available $(Ba,Sr)_2SiO_4$:Eu^{2+} (570 nm) phosphors. These results indicate that for high power LED applications, SMYP:$0.01Eu^{2+}$ and SMLP:$0.03Eu^{2+}$ are promising yellow-emitting phosphors. As seen in the Figure 5 insets, the relationship of the relative emission intensities with temperature can be used to calculate the activation energy (E_a) from thermal quenching using the following equation:[25]

$$\ln\left(\frac{I_0}{I}\right) = \ln A - \frac{E_a}{k_B T} \quad (1)$$

where I_0 and I are the luminescence intensity of the SMYP:$0.01Eu^{2+}$ or SMLP:$0.03Eu^{2+}$ phosphor at room temperature and the testing temperature, respectively, A is a constant, and k_B is the Boltzmann constant (8.617×10^{-5} eV/K). The E_a was calculated to be 0.1274 and 0.1544 eV for the SMYP:$0.01Eu^{2+}$ and SMLP:$0.03Eu^{2+}$ phosphors, respectively. These results demonstrated that the SMYP:$0.01Eu^{2+}$ phosphor has higher thermal stability than the SMLP:$0.03Eu^{2+}$ phosphor.

3.5. Optical Properties, LED Lamp Fabrication, and EL Spectrum. As shown in Figure 6 and Table 1, the CIE chromaticity diagram, CIE chromaticity coordinates, CCT, and *Ra* were

Table 1. CIE Chromaticity Coordinates, CCT, and *Ra* for Two Blends of $Sr_8MgLn(PO_4)_7$:Eu^{2+} (Ln = Y, La) and $BaMgAl_{10}O_{17}$:Eu^{2+} under 400 nm Excitation

	$Sr_8MgY(PO_4)_7$:$0.01Eu^{2+}$				$Sr_8MgLa(PO_4)_7$:$0.03Eu^{2+}$		
	(*x*, *y*)	CCT (K)	*Ra*		(*x*, *y*)	CCT (K)	*Ra*
01	(0.419, 0.444)	3608	87.07	11	(0.479, 0.454)	2762	82.07
02	(0.400, 0.416)	3800	91.26	12	(0.462, 0.434)	2848	84.55
03	(0.382, 0.391)	4048	94.37	13	(0.430, 0.397)	3064	88.47
04	(0.370, 0.374)	4290	95.40	14	(0.410, 0.373)	3247	90.74
05	(0.358, 0.357)	4574	95.55	15	(0.399, 0.360)	3378	91.48
06	(0.347, 0.343)	4877	94.78	16	(0.390, 0.351)	3505	92.33
07	(0.333, 0.324)	5471	92.59	17	(0.373, 0.331)	3835	92.13
08	(0.320, 0.306)	6267	89.25	18	(0.358, 0.314)	4215	90.82
09	(0.304, 0.284)	7824	85.11	19	(0.341, 0.295)	4952	86.91
10	(0.288, 0.263)	10890	81.27	20	(0.329, 0.281)	5735	82.79

determined for blends of either yellow-emitting SMYP:$0.01Eu^{2+}$ (points 01 to 10) or SMLP:$0.03Eu^{2+}$ (points 11 to 20) with blue-emitting $BaMgAl_{10}O_{17}$:Eu^{2+} (BAM:Eu^{2+}) phosphors under 400 nm excitation. For the mixture of the SMYP:$0.01Eu^{2+}$ and BAM:Eu^{2+} phosphors, the color tone and chromaticity coordinates (*x*, *y*) can be tuned from yellow (point 01, (0.419, 0.444)) through to white (point 07, (0.333, 0.324)) and eventually to cool white (point 10, (0.288, 0.263)). Accordingly, the correlated color temperature and color-rendering index can be tuned from warm yellow light (3608 K, 87.07) through white light (5471 K, 92.59) to cool white light (10,890 K, 81.27). By weight ratio tuning, the outputs of the SMLP:$0.03Eu^{2+}$ and BAM:Eu^{2+} phosphors were found to systematically shift to the blue region with increasing BAM:Eu^{2+} weight ratio. The emission hue, CIE, CCT, and *Ra* were found to be tunable from yellow (point 11, CIE = (0.333, 0.324), CCT = 2762 K, *Ra* = 82.07) to white (point 20, CIE = (0.329, 0.281), CCT = 5735 K, *Ra* = 82.79) in the visible spectral region. The CRI gradually increases with the BAM:Eu^{2+} phosphor mixed ratio and reaches a maximum at 95.55 (point 05) and 92.33 (point 16), after which it decreases with an increase in the BAM:Eu^{2+} mixed ratio. The results indicate that the blends of SMYP:$0.01Eu^{2+}$ or SMLP:$0.03Eu^{2+}$ phosphor with BAM:Eu^{2+} had suitable colors, and CCT and *Ra* values were suitable for application in white-light near-UV LEDs.

Figures 7a−b shows the electroluminescent (EL) spectra of white-light near-UV LEDs driven by a current of 350 *m*A. The white-light near-UV LEDs were fabricated by a mixture of transparent silicon resin, yellow-emitting SMYP:$0.01Eu^{2+}$ or SMLP:$0.03Eu^{2+}$, and blue-emitting BAM:Eu^{2+} phosphors, which were dropped onto a 400 nm near-UV chip. The EL spectra clearly show near-UV bands at around 400 nm, blue-emitting bands corresponding to the BAM:Eu^{2+} phosphor at around 454 nm, and yellow-emitting bands corresponding to the SMYP:$0.01Eu^{2+}$ phosphors at around 514 and 601 nm (Figure 7a), or the SMLP:$0.03Eu^{2+}$ at around 604 nm (Figure 7b). The optical properties of the white-light near-UV LEDs shown in Figure 7a have CIE color coordinates of (0.348, 0.357) at a warm white light CCT of 4705 K and an excellent *Ra* of 95.375. Figure 7b shows CIE color coordinates of (0.365, 0.328), a warm white light CCT of 4100 K, and a *Ra* of 91.75. The full set of the CRIs and the average CRIs, *Ra*, are listed in Table 2. The SMYP:$0.01Eu^{2+}$-phosphor-converted white-light near-UV LEDs show a higher CCT of 4705 K and *Ra* of 95.375, compared to

dx.doi.org/10.1021/ic200515w |*Inorg. Chem.* 2011, 50, 5725–5730

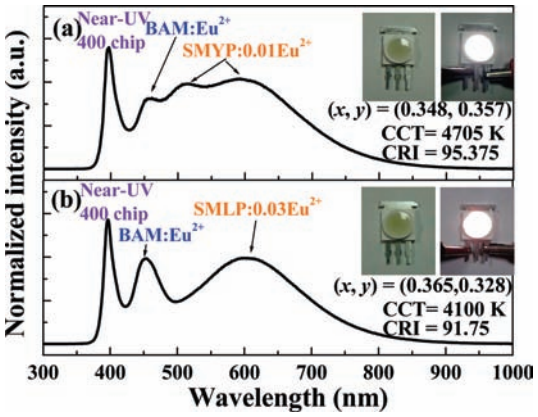

Figure 7. EL spectra of white-LED lamps fabricated using a near-UV 400 nm chip combined with a blend of (a) blue-emitting $BaMgAl_{10}O_{17}:Eu^{2+}$ and yellow-emitting $Sr_8MgY(PO_4)_7:0.01Eu^{2+}$ phosphors or (b) blue-emitting $BaMgAl_{10}O_{17}:Eu^{2+}$ and yellow-emitting $Sr_8MgLa(PO_4)_7:0.03Eu^{2+}$ phosphors. The inset shows the photograph of the LED lamp package driven by a 350 *m*A current.

Table 2. Full Set of 8 Components of the CRIs and the *Ra* of a 400 nm near-UV Chip Pumped with $SMYP:0.01Eu^{2+}$ + $BAM:Eu^{2+}$ and $SMLP:0.03Eu^{2+}$ + $BAM:Eu^{2+}$ Phosphors

white-light LED	R1	R2	R3	R4	R5	R6	R7	R8	*Ra*
$SMYP:0.01Eu^{2+}$ + $BAM:Eu^{2+}$	94	97	97	94	95	98	95	93	95.38
$SMLP:0.03Eu^{2+}$ + $BAM:Eu^{2+}$	94	93	92	92	94	90	89	90	91.75

$SMLP:0.03Eu^{2+}$ phosphor, which has a CCT of 4100 K and an *Ra* of 91.75 because of the increased green light (514 nm) in the $SMYP:0.01Eu^{2+}$ phosphor EL spectra. The inset of Figures 7a−b shows the appearance of the phosphor-converted white-LED lamps and the white-light emission from the LEDs driven by a 350 *m*A current. In comparison with the blue InGaN chip pumped with $YAG:Ce^{3+}$ phosphor (*Ra* = 75, CCT = 7756 K),[8] the white-light near-UV LEDs fabricated in this study show higher *Ra* values (*Ra* = 95.375 for $SMYP:0.01Eu^{2+}$, 91.75 for $SMLP:0.03Eu^{2+}$) and lower CCT values (CCT = 4705 K for $SMYP:0.01Eu^{2+}$, 4100 K for $SMLP:0.03Eu^{2+}$). Therefore, the $SMYP:0.01Eu^{2+}$ and $SMLP:0.03Eu^{2+}$ phosphors are promising for application in excellent CRI and tunable CCT white-light near-UV LEDs.

4. CONCLUSIONS

In summary, two novel yellow-emitting phosphors, $Sr_8MgY(PO_4)_7:xEu^{2+}$ and $Sr_8MgLa(PO_4)_7:yEu^{2+}$, have been reported. The excitation spectra show broad band excitation in the 250−450 nm near-ultraviolet region, which matches well with near-UV chips. The emission spectra of the $Sr_8MgY(PO_4)_7:Eu^{2+}$ and $Sr_8MgLa(PO_4)_7:Eu^{2+}$ phosphors exhibit strong yellow emissions centered at 518, 610, and 611 nm with CIE chromaticity coordinates of (0.440, 0.471) and (0.495, 0.473), respectively. The optimum concentrations of Eu^{2+} in the $Sr_8MgY(PO_4)_7:Eu^{2+}$ and $Sr_8MgLa(PO_4)_7:Eu^{2+}$ phosphors were determined to be 0.01 and 0.03 mol and the band gaps were estimated to be about 3.2 and 3.17 eV, respectively. The warm white-emitting near-UV LEDs with mixed phosphors of $BAM:Eu^{2+}$ and either $Sr_8MgY(PO_4)_7:0.01Eu^{2+}$ or $Sr_8MgLa(PO_4)_7:0.03Eu^{2+}$ showed excellent CRIs of 95.375 and 91.75, warm correlated color temperatures of 4705 and 4100 K, and CIE chromaticity coordinates of (0.348, 0.357) and (0.365, 0.328), respectively. The results of our investigation indicate that synthesized warm-white-emitting near-UV LEDs exhibit excellent CRI and lower CCT compared to those of conventional white LEDs based on $YAG:Ce^{3+}$ pumped with blue LED chips (CIE = (0.292, 0.325), CRI = 75, CCT = 7756 K).[8] Therefore, our novel yellow-emitting $Sr_8MgY(PO_4)_7:0.01Eu^{2+}$ and $Sr_8MgLa(PO_4)_7:0.03Eu^{2+}$ phosphors can serve as key materials for phosphor-converted white-light near-UV LEDs.

■ ASSOCIATED CONTENT

Supporting Information. Further details are given in Figure S1. This material is available free of charge via the Internet at http://pubs.acs.org.

■ AUTHOR INFORMATION

Corresponding Author

*Phone: +886-35731695. E-mail: tmchen@mail.nctu.edu.tw.

■ ACKNOWLEDGMENT

This research was supported by National Science Council of Taiwan under contract No. NSC98-2113-M-009-005-MY3.

■ REFERENCES

(1) Kim, J. S.; Jeon, P. E.; Choi, J. C.; Park, H. L.; Mho, S. I.; Kim, G. C. *Appl. Phys. Lett.* **2004**, *84*, 2931.
(2) Im, W. B.; Kim, Y. I.; Fellows, N. N.; Masui, H.; Hirata, G. A.; Den, S. P.; Seshadri, B. R. *Appl. Phys. Lett.* **2008**, *93*, 091905.
(3) Nishida, T.; Ban, T.; Kobayashi, N. *Appl. Phys. Lett.* **2003**, *82*, 3817.
(4) Shur, M. S.; Žukauskas, A. *Proc. IEEE* **2005**, *93*, 1691–1703.
(5) Wang, F.; Xue, X.; Liu, X. *Angew. Chem., Int. Ed.* **2008**, *47*, 906–909.
(6) Uchida, Y.; Taguchi, T. *Opt. Eng.* **2005**, *44*, 124003.
(7) Bachmann, V.; Ronda, C.; Meijerink, A. *Chem. Mater.* **2009**, *21*, 2077–2084.
(8) Jang, H. S.; Won, Y. H.; Jeon, D. Y. *Appl. Phys. B: Laser Opt.* **2009**, *95*, 715–720.
(9) Setlur, A. A.; Heward, W. J.; Gao, Y.; Srivastava, A. M.; Chandran, R. G.; Shankar, M. V. *Chem. Mater.* **2006**, *18*, 3314–3322.
(10) Song, W. S.; Kim, Y. S.; Yang, H. *Mater. Chem. Phys.* **2009**, *117*, 500–503.
(11) Wang, Z. J.; Li, P. L.; Yang, Z. P.; Guo, Q. L.; Li, X. *Chin. Phys. B* **2010**, *19*, 017801.
(12) Yang, Z.; Wang, S.; Yang, G.; Tian, J.; Li, P.; Li, X. *Mater. Lett.* **2007**, *61*, 5258–5260.
(13) Saradhi, M. P.; Varadaraju, U. V. *Chem. Mater.* **2006**, *18*, 5267–5272.
(14) Lee, J. H.; Kim, Y. J. *Mater. Sci. Eng., B* **2008**, *146*, 99–102.
(15) Liu, J.; Lian, H.; Shi, C.; Sun, J. *J. Electrochem. Soc.* **2005**, *152*, G880–G884.
(16) Wu, Z.; Gong, M.; Shi, J.; Wang, G.; Su, Q. *Chem. Lett.* **2007**, *36*, 410–411.
(17) Tang, Y. S.; Hu, S. F.; Ke, W. C.; Lin, C. C.; Bagkar, N. C.; Liu, R. S. *Appl. Phys. Lett.* **2008**, *93*, 131114.
(18) Belik, A. A.; Izumi, F.; Ikeda, T.; Okui, M.; Malakho, A. P.; Morozov, V. A.; Lazoryak, B. I. *J. Solid State Chem.* **2002**, *168*, 237–244.
(19) ICSD file No. 59722.
(20) Shinde, K. N.; Nagpure, I. M.; Dhoble, S. J. *Synth. React. Inorg., Met.-Org., Nano-Met. Chem.* **2011**, *41*, 107–113.

(21) Vyssotsy, V. A.; Gordon, S. B.; Frisch, H. L.; Hammersley, J. M. *Phys. Rev.* **1961**, *123*, 1566–1567.
(22) Kuo, T. W.; Huang, C. H.; Chen, T. M. *Opt. Express* **2010**, *18*, A231–A236.
(23) Zhang, X.; Chen, H.; Ding, W.; Wu, H.; Kim, J. *J. Am. Ceram. Soc.* **2009**, *92*, 429–432.
(24) Zhang, Q.; Wang, J.; Yu, R.; Zhang, M.; Su, Q. *Electrochem. Solid-State Lett.* **2008**, *11*, H335–H337.
(25) Huang, C. H.; Liu, W. R.; Chen, T. M. *J. Phys. Chem. C* **2010**, *114*, 18698–18701.